Dopamine transporter phosphorylation site threonine 53 is stimulated by amphetamines and regulates dopamine transport, efflux, and cocaine analog binding

Received for publication, March 17, 2017, and in revised form, August 29, 2017 Published, Papers in Press, September 22, 2017, DOI 10.1074/jbc.M117.787002

Sathya Challasivakanaka[‡], Juan Zhen[§], Margaret E. Smith[‡], Maarten E. A. Reith[§¶], James D. Foster[‡], and Roxanne A. Vaughan[‡1]

From the [‡]Department of Biomedical Sciences, University of North Dakota School of Medicine and Health Sciences, Grand Forks, North Dakota 58201 and the Departments of [§]Psychiatry and [¶]Biochemistry and Molecular Pharmacology, New York University School of Medicine, New York, New York 10016

Edited by Paul E. Fraser

The dopamine transporter (DAT) controls the spatial and temporal dynamics of dopamine neurotransmission through reuptake of extracellular transmitter and is a target for addictive compounds such as cocaine, amphetamine (AMPH), and methamphetamine (METH). Reuptake is regulated by kinase pathways and drug exposure, allowing for fine-tuning of clearance in response to specific conditions, and here we examine the impact of transporter ligands on DAT residue Thr-53, a proline-directed phosphorylation site previously implicated in AMPH-stimulated efflux mechanisms. Our findings show that Thr-53 phosphorylation is stimulated in a transporter-dependent manner by AMPH and METH in model cells and rat striatal synaptosomes, and in striatum of rats given subcutaneous injection of METH. Rotating disc electrode voltammetry revealed that initial rates of uptake and AMPH-induced efflux were elevated in phosphorylation-null T53A DAT relative to WT and charge-substituted T53D DATs, consistent with functions related to charge or polarity. These effects occurred without alterations of surface transporter levels, and mutants also showed reduced cocaine analog binding affinity that was not rescued by Zn^{2+}. Together these findings support a role for Thr-53 phosphorylation in regulation of transporter kinetic properties that could impact DAT responses to amphetamines and cocaine.

The dopamine transporter (DAT)[2] is an integral plasma membrane protein expressed in dopaminergic neurons that translocates dopamine (DA) from the extracellular space into the presynaptic terminal and is a major factor in spatial and temporal control of DA signaling (1). DAT is a primary target for psychostimulant drugs that elevate extracellular DA including inhibitors such as cocaine that block reuptake, and substrates such as amphetamine (AMPH) and methamphetamine (METH) that stimulate efflux of intracellular transmitter (2). Uptake and efflux activities are tightly regulated by signaling pathways including protein kinase C (PKC) and extracellular signal–regulated kinase (ERK), providing for acute modulation of reuptake in response to physiological demands (3–6). Dysregulation of these processes has been hypothesized to contribute to DA imbalances in disorders such as Parkinson's disease, bipolar disorder, attention deficit hyperactivity disorder, and dopamine transporter deficiency syndrome (7), with recent studies supporting DAT regulatory alterations in some of these conditions (8–10).

Our group has shown that rat (r) DAT undergoes PKC- and AMPH-stimulated phosphorylation on a cluster of serine residues at the distal end of the cytoplasmic N terminus (6, 11–13), and numerous studies have examined the roles of these sites in AMPH- and kinase-mediated regulation of uptake and efflux (14, 15). More recently we demonstrated that threonine 53 in the membrane proximal region of the N terminus also undergoes PKC- and phosphatase-dependent phosphorylation (16). This site, which is conserved as a Thr in mouse DAT and a Ser in human DAT, is followed by a proline, making it a substrate for kinases such as mitogen-activated protein kinases (MAPKs), cyclin-dependent kinases (CDKs), and glycogen-synthase kinases that require a Pro immediately C-terminal to the phosphoacceptor (17, 18). Our previous analyses showed that phosphorylation-null Thr-53 → alanine (Ala) and charge-substituted Thr-53 → aspartate (Asp) mutants possessed reduced [^{3}H]DA transport V_{max} and essentially complete loss of AMPH-stimulated [^{3}H]1-methyl-4-phenylpyridinium (MPP^+) efflux (16), implicating this residue in mechanisms of forward and reverse transport.

Here we further characterize the relationship between Thr-53 and psychostimulant drug mechanisms by examining phosphorylation responses to transporter substrates and blockers. Our findings show that Thr-53 phosphorylation is not affected by cocaine or other inhibitors but is rapidly stimulated by AMPH and METH in model cells and rat striatal synaptosomes, and in striatal tissue of rats injected with METH. Anal-

This work was supported by National Institutes of Health Grants DA013147 (to R. A. V.), DA031991 (to J. D. F.), DA019676 (to M. E. A. R.), and a University of North Dakota Doctoral Summer Fellowship (to S. C.). The authors declare that they have no conflicts of interest with the contents of this article. The content is solely the responsibility of the authors and does not necessarily represent the official views of the National Institutes of Health.

[1] To whom correspondence should be addressed: 1301 N. Columbia Rd., Grand Forks, ND 58201. Tel.: 701-777-3419; Fax: 701-777-2382; E-mail: roxanne.vaughan@med.und.edu.

[2] The abbreviations used are: DAT, dopamine transporter; DA, dopamine; AMPH, amphetamine; METH, methamphetamine; CFT, (–)2β-carbomethoxy-3β-(4-fluorophenyl)tropane; MPP^+, [^{3}H]1-methyl-4-phenylpyridinium; RDEV, rotating disc electrode voltammetry; $LLCPK_1$, Lewis lung carcinoma-porcine kidney; CDK, cyclin-dependent kinase; BZT, benztropine; OA, okadaic acid; SH, Src homology; SP, sucrose phosphate; ANOVA, analysis of variance.

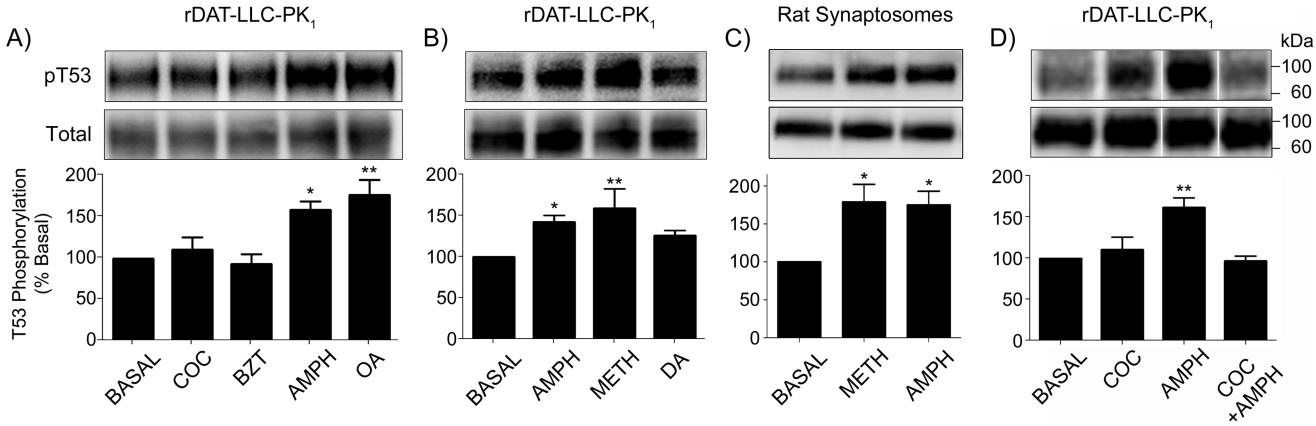

Figure 1. AMPH and METH stimulate Thr-53 phosphorylation by a cocaine-sensitive mechanism. rDAT-LLCPK$_1$ cells were treated for 30 min with vehicle or: *A,* (–)-cocaine (*COC*) (10 μM), BZT (10 μM), AMPH (10 μM), or OA (1 μM); *B,* AMPH, METH, or DA (all 10 μM); or *D,* the indicated combinations of AMPH (10 μM) and cocaine (100 μM). *C,* rat striatal synaptosomes were treated with vehicle, 10 μM AMPH or 10 μM METH. Equal amounts of protein were analyzed for Thr-53 phosphorylation (*upper panels*) or total DAT (*lower panels*). *Vertical white dividing lines* in blots indicate the removal of intervening lanes from the same gel. Histograms show quantification of Thr-53 phosphorylation (% basal, mean ± S.E. of 9 (*A*) or 4 (*B–D*) independent experiments). *, $p < 0.05$; **, $p < 0.01$ *versus* basal (one-way ANOVA, with Tukeys' post-hoc test). Molecular mass markers for all gels are shown on the *right*.

ysis of transporter properties by rotating disc electrode voltammetry (RDEV) showed that initial velocities of DA uptake and AMPH-stimulated DA efflux are increased in T53A DAT relative to WT and T53D DATs, supporting a role for phosphorylation in regulation of these functions. The mutant forms showed no differences from the WT protein in AMPH transport inhibition potency, and no changes in surface levels under efflux assay conditions, indicating that altered functions follow from changes in kinetic parameters. T53A DAT also showed reduced cocaine analog binding affinity, which was not rescued by Zn^{2+}. These findings support a role for Thr-53 phosphorylation in regulation of DAT kinetic properties that may impact transporter responsiveness to amphetamines and cocaine.

Results

Psychostimulant substrates stimulate Thr-53 phosphorylation

In all phosphorylation experiments Thr-53 modification was assessed using a highly specific antibody developed against the phosphorylated form of this site (16), and signals obtained were normalized to the amount of total DAT protein assessed in parallel using a pan monoclonal antibody (20). None of the treatments examined had any effect on total DAT levels, indicating that changes in phospho (p)Thr-53 signals arise from stoichiometric alterations of phosphorylation.

To examine the effects of substrates and blockers on Thr-53 phosphorylation, we treated rDAT-LLCPK$_1$ cells for 30 min with vehicle, (–)-cocaine, benztropine (BZT), or AMPH (all 10 μM), using 1 μM okadaic acid (OA), a phosphatase inhibitor previously shown to increase Thr-53 phosphorylation (16), as a positive control (Fig. 1*A*). With vehicle treatment Thr-53 displayed a basal level of phosphorylation that reflects the tonic rate of phosphate turnover, and no change in this level was detected when cells were exposed to the typical or atypical transport blockers cocaine (110 ± 15% of basal, $p > 0.05$) or BZT (93 ± 13% of basal, $p > 0.05$) (Fig. 1*A*), or in other experiments to 10 μM GBR 12909 or 10 μM rimcazole (not shown). In contrast, phosphorylation of Thr-53 was significantly increased by AMPH (152 ± 9% of basal, $p < 0.05$), similar to levels induced by OA (177 ± 19% of basal, $p < 0.01$).

Characterization of additional substrates in rDAT-LLCPK$_1$ cells showed that Thr-53 phosphorylation was increased by AMPH (142 ± 8% of basal, $p < 0.05$) and METH (159 ± 24% of basal, $p < 0.01$), with a possible trend toward enhanced phosphorylation induced by DA (125 ± 6% of basal) (Fig. 1*B*). Similar responses were seen in rat striatal synaptosomes, with Thr-53 phosphorylation increased by both AMPH (175 ± 18% of basal, $p < 0.05$) and METH (179 ± 23% of basal, $p < 0.05$) (Fig. 1*C*). To determine whether the effect of amphetamines was due to diffusion through the plasma membrane (24) or to transport or binding to DAT, we pretreated rDAT-LLCPK$_1$ cells with 100 μM (–)-cocaine prior to addition of 10 μM AMPH (Fig. 1*D*). When drugs were applied separately, pThr-53 levels were stimulated by AMPH (154 ± 6% of basal, $p < 0.01$) but not cocaine (111 ± 16% of basal, $p > 0.05$), and when cells were pre-treated with cocaine prior to application of AMPH, no phosphorylation increase was observed (97 ± 6% of basal, $p > 0.05$), indicating that the AMPH effect occurs through a DAT-dependent mechanism.

Time course of AMPH/METH-stimulated Thr-53 phosphorylation

Characterization of the Thr-53 response to drugs for various periods of time between 1 and 60 min showed that treatment of rDAT-LLCPK$_1$ cells with 10 μM AMPH (Fig. 2*A*) induced a gradual increase in Thr-53 phosphorylation that reached the highest levels (143 ± 8% of basal, $p < 0.01$ and 139 ± 8% of basal, $p < 0.05$) between 30 and 60 min. 10 μM METH (Fig. 2*B*) also induced a gradual response that peaked by 20–30 min (123 ± 2% of basal, $p < 0.01$ and 131 ± 4% of basal, $p < 0.001$). In contrast, METH stimulation of Thr-53 phosphorylation in synaptosomes occurred much more rapidly (Fig. 2*C*), with apparent maximal increases obtained within 1 min of drug application (133 ± 3% of basal, $p < 0.01$) and sustained through 10 (128 ± 3% of basal, $p < 0.01$) and 20 min (121 ± 7% of basal, $p < 0.01$) (not shown). The slower development of Thr-53 phosphorylation in LLCPK$_1$ cells than in synaptosomes may follow from different complements of kinases and phosphatases, or from other factors that may impact the apparent time course

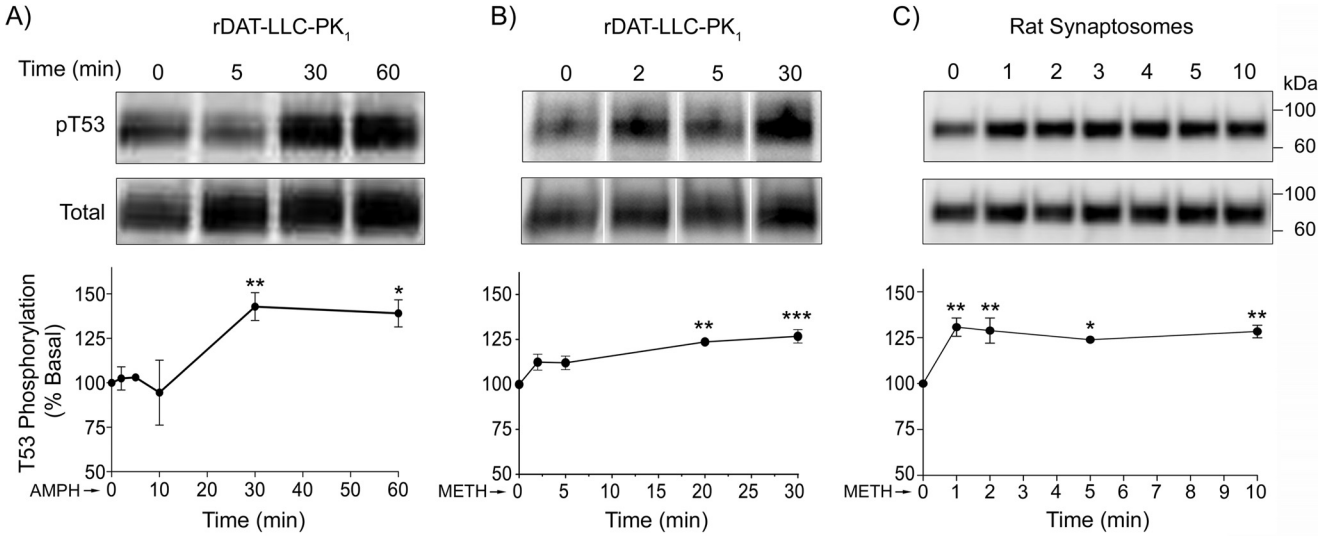

Figure 2. Time course of Thr-53 phosphorylation in cells and synaptosomes. rDAT-LLCPK$_1$ cells (*A* and *B*) and rat striatal synaptosomes (*C*) were treated for the indicated times with 10 μM AMPH (*A*) or 10 μM METH (*B* and *C*), and equal amounts of protein were analyzed for Thr-53 phosphorylation (*upper panels*) or total DAT (*lower panels*). *Vertical white dividing lines* in blots indicate the removal of intervening lanes from the same gel. Graphs show quantification of Thr-53 phosphorylation (% basal, mean ± S.E. for each time point, $n = 3$–5). *, $p < 0.05$; **, $p < 0.01$; ***, $p < 0.001$ (one-way ANOVA, with Tukeys post hoc test).

such as transporter expression levels or relative phosphorylation of total and surface transporters.

METH stimulates pThr-53 in vivo

To determine whether drug-induced phosphorylation changes occur in the brain, we administered single subcutaneous injections of saline, cocaine (15 mg/kg), or METH (15 mg/kg) to rats and harvested striatal tissue 30 min after injection (Fig. 3*A*). In animals that received saline, Thr-53 showed a tonic level of phosphorylation, and this was not changed when animals were injected with cocaine (97 ± 4% of basal, $p > 0.05$), paralleling results from *in vitro* studies, but in animals that received METH, Thr-53 phosphorylation was significantly increased (130 ± 10% of basal, $p < 0.05$), demonstrating the regulation of this site *in vivo*. Time course analysis of the response (Fig. 3*B*) showed that Thr-53 phosphorylation was increased within 10 min of METH injection (119 ± 4% of basal, $p < 0.01$) and remained elevated through 30 (129 ± 10% of basal, $p < 0.05$) and 60 min (128 ± 10% of basal, $p < 0.05$), indicating a rapid and sustained response upon entry of the drug into the brain.

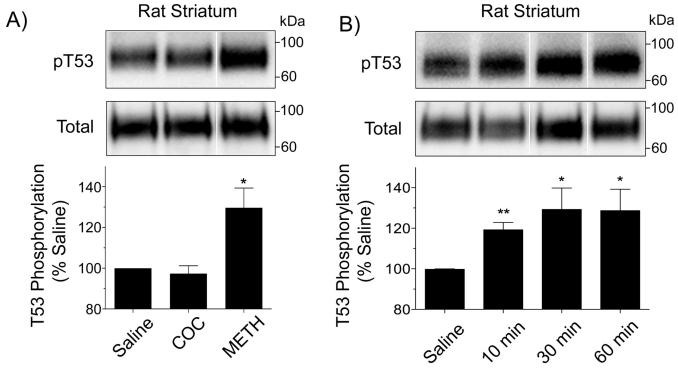

Figure 3. METH stimulates Thr-53 phosphorylation *in vivo*. *A,* male Sprague-Dawley rats were given subcutaneous injections of (*A*) saline, (–)-cocaine (15 mg/kg), or METH (15 mg/kg) and decapitated after 30 min, or (*B*) saline or METH (15 mg/kg) and decapitated at the indicated time points. Striatal membranes were harvested and equal amounts of protein analyzed for Thr-53 phosphorylation (*upper panels*) or total DAT (*lower panels*). *Vertical white dividing lines* in blots indicate the removal of intervening lanes from the same gel. Histograms show quantification of Thr-53 phosphorylation (% basal, mean ± S.E., *, $p < 0.05$; **, $p < 0.01$, $n = 3$–5); *A*, one-way ANOVA, with Tukey's post hoc test; *B*, Student's *t* test.

T53A DAT displays altered transport and efflux kinetics

In previous analyses of Thr-53 function we used radioisotope assays to examine kinetic characteristics of T53A and T53D DAT mutants (16). These forms are active for transport, sensitive to cocaine and AMPH, and show total and surface expression of ~60–70% of the WT DAT levels (16). Results from these previous studies indicated that steady-state [^{3}H]DA transport capacities of the T53A and T53D forms normalized for DAT surface levels were ~50% of the WT DAT level and that AMPH-stimulated efflux of [^{3}H]MPP$^+$ was essentially abolished (16), implicating a role for the residue in regulation of transport and efflux properties.

In the current study we sought to further characterize Thr-53 transport mechanisms specifically related to DA using RDEV (21). Fig. 4, *A* and *B,* show representative RDEV traces for WT, T53A, and T53D DATs performed using 0.25 and 1 μM DA, and summarized kinetic values obtained using 0.25–10 μM DA are presented in Table 1. The findings show that T53A DAT possesses elevated uptake V_{max} compared with the WT transporter (64.6 ± 10.9 *versus* 28.2 ± 5.7 pmol/s/mg, $p < 0.05$), with T53D DAT possessing an intermediate value (43.8 ± 9.7 pmol/s/mg) that is not statistically different from either (Table 1). These are absolute values not corrected for the lower surface expression of the mutants, and the differences between the forms may thus be somewhat greater. DA K_m values between the forms were not significantly different.

Once DA accumulation in the cells reached steady-state levels (2–5 min), 10 μM AMPH was applied to stimulate efflux. T53A and T53D DATs displayed clearly detectable efflux as demonstrated in the RDEV traces (Fig. 4, *A* and *B*) and in Table

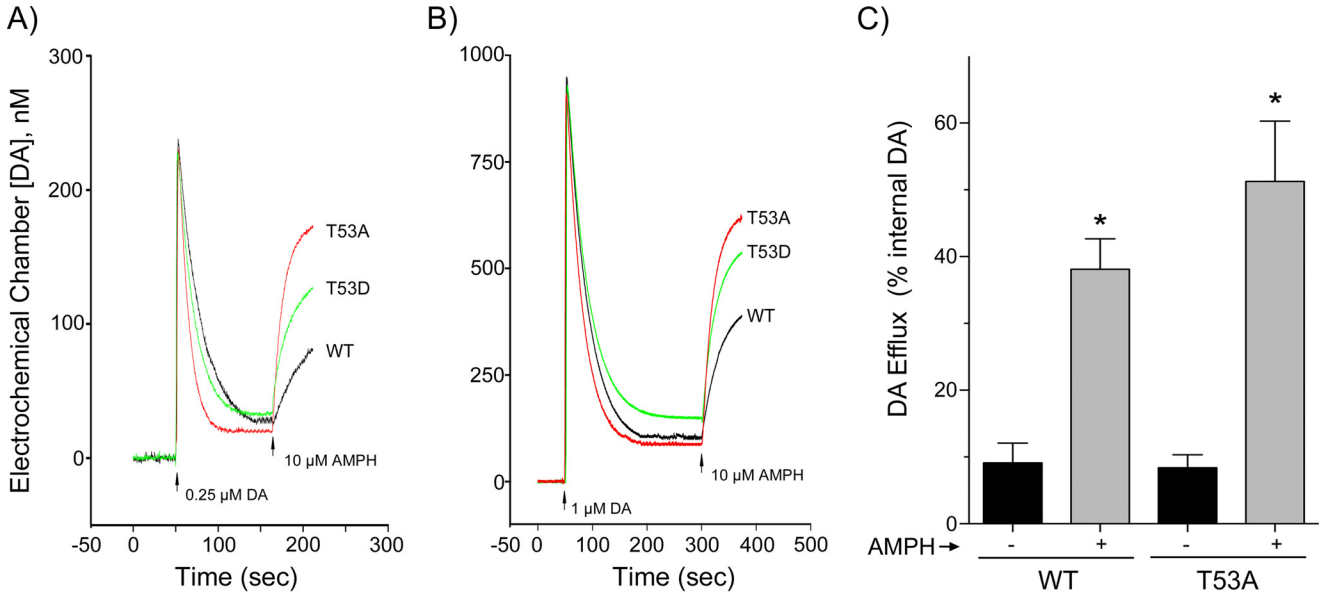

Figure 4. Uptake and efflux analyses of T53A and T53D DATs. *A* and *B*, RDEV analysis of DA uptake and efflux. Superimposed representative traces WT DAT (black line), T53A DAT (*red line*), and T53D DAT (*green line*) show clearance of (*A*) 0.25 μM DA and (*B*) 1 μM DA, followed by application of 10 μM AMPH (*arrow*) to induce DA release. Kinetic values obtained from replicate experiments using 0.25–10 μM DA are presented in Table 1. *C*, WT- and T53A-LLCPK$_1$ cells loaded with [^{3}H]DA were treated with vehicle or 10 μM AMPH for 5 min. Histogram shows amount of radioactivity (% of internal DA) collected in supernatants of each form (mean ± S.E. of 3 independent experiments), *, $p < 0.05$ *versus* vehicle for each form by Student's *t* test.

Table 1

Kinetic properties of DAT Thr-53 mutants

WT, T53A, and T53D DAT forms were analyzed by RDEV to determine Michaelis constant (K_m) and maximal velocity (V_{max}) for DA uptake and AMPH-induced DA efflux. Results are expressed as mean ± S.E. from $n = 4$ (T53A) or $n = 5$ (WT and T53D) independent experiments.

Cells	DA uptake		AMPH-induced DA efflux		V_{max} efflux/ V_{max} uptake
	V_{max}	K_m	V_{max}	K_m	
	pmol/s/mg	μM	*pmol/s/mg*	μM	
WT	28.2 ± 5.7	1.83 ± 0.38	15.2 ± 2.1	446 ± 116	0.72 ± 0.23
T53A	64.6 ± 10.9[a]	3.05 ± 0.73	81.4 ± 6.7[a]	743 ± 136[a]	1.46 ± 0.17[a]
T53D	43.8 ± 9.7	1.86 ± 0.34	25.2 ± 5.2[b]	389 ± 60[b]	0.49 ± 0.06[b]

[a] $p < 0.05$, T53A DAT *vs.* WT DAT.
[b] $p < 0.05$, T53D DAT *vs.* T53A DAT (one-way ANOVA followed by Holm-Sidak post hoc test).

1. Compared with the WT protein, T53A DAT showed elevated DA efflux V_{max} (81.4 ± 6.7 *versus* 15.2 ± 2.1 pmol/s/mg, $p < 0.05$) and increased DA K_m (743 ± 136 *versus* 446 ± 116 μM, $p < 0.05$). Efflux V_{max} (25.2 ± 5.2 pmol/s/mg) and K_m (389 ± 60 μM) for T53D DAT were significantly different from those of T53A DAT (both $p < 0.05$) (Table 1), but not from the WT protein, suggesting that normal responsiveness is maintained by polarity or negative charge at the site.

As the velocity of substrate-induced efflux depends on the uptake velocity of the inducer, which can vary for each mutation (21, and see "Experimental procedures" for more detail), we also considered the ratio of efflux to uptake V_{max} for each of the forms (Table 1). This ratio was significantly greater for T53A DAT (1.46 ± 0.17) than for WT DAT (0.72 ± 0.23, $p < 0.05$) or T53D DAT (0.49 ± 0.06, $p < 0.05$), further supporting enhanced efflux capacity in the T53A form. Examination of these ratios at multiple internal DA concentrations (5-5000 μM) showed that efflux mediated by T53A DAT is always enhanced relative to the WT protein (3.2-fold at 5 μM to 5.1-fold at 5000 μM), indicating the effect of the mutation over a wide range of intracellular substrate levels.

Because these results differed significantly from our previous studies in which we found essentially complete loss of AMPH-stimulated [^{3}H]MPP$^+$ efflux in T53A and T53D DATs using perfusion analysis (16), we also examined the ability of T53A DAT to mediate [^{3}H]DA efflux in batch treatment conditions of plated cells (Fig. 4*B*). For these experiments WT and T53A DAT cells were loaded with [^{3}H]DA and assessed for basal and AMPH-stimulated release over a period of 5 min. In vehicle conditions, WT and T53A DAT cells released 9.1 ± 3.0 and 8.4 ± 2.0% of intracellular [^{3}H]DA, respectively, and in the presence of AMPH released 38.1 ± 4.6 and 51.3 ± 9.0% of intracellular [^{3}H]DA, respectively (both $p < 0.05$ *versus* basal), confirming the ability of the mutant to support both basal and AMPH-stimulated reverse transport.

To determine whether differential efflux in the forms could result from altered responses to AMPH or to differential trafficking in response to DA during the cell loading phase, we examined the forms for AMPH-inhibition of uptake and for changes in transporter surface expression (Fig. 5). AMPH concentration-response experiments showed no difference in AMPH potencies for any of the forms (Fig. 5*A*), with equivalent levels of inhibition obtained at 10 μM AMPH, the concentration used to stimulate efflux, indicating that differential efflux did not result from mutation-induced impacts on this property. To determine whether plasma membrane levels of transporters

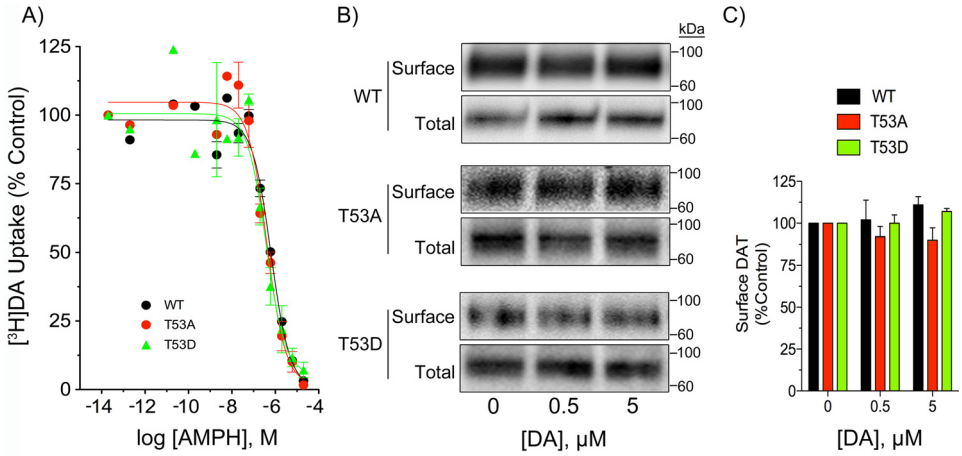

Figure 5. AMPH concentration-dependence and surface biotinylation of WT, T53A, and T53D DATs. *A,* LLCPK$_1$ cells expressing WT, T53A, or T53D DATs were analyzed for [^{3}H]DA transport in the presence of the indicated concentrations of AMPH. Results are expressed as % control for each form and represent mean ± S.E. of three independent experiments. *B,* LLCPK$_1$ cells expressing the indicated DAT forms were treated with vehicle, 0.5 μM DA, or 5 μM DA for 5 min and subjected to surface biotinylation. Equal amounts of protein for each form were analyzed for total and surface DAT levels. Quantification of surface levels for each form normalized to vehicle control is shown in *panel C*.

changed during the DA loading phase of the RDEV procedure we treated cells with 0.5 or 5 μM DA for 5 min and performed cell surface biotinylation (Fig. 5*B*). Quantification of the results (Fig. 5*C*) showed no changes in surface DAT levels with DA treatments, indicating that the enhanced efflux capacity of T53A occurs via a kinetic alteration of the transporter.

CFT binding analyses

Our findings that T53A DAT exhibited altered uptake and efflux parameters without obvious changes in surface levels suggest that the mutation impacts the rate of transporter cycling through outwardly and inwardly facing conformations during the substrate translocation process (25). It is thought that [^{3}H]CFT binding is favored by the outwardly facing conformation (26), and that Zn^{2+} stimulation of binding reflects stabilization of outward forms (27). Saturation binding performed across 1–100 nM (–)2β-carbomethoxy-3β-(4-fluorophenyl)tropane (CFT) produced typical curvilinear profiles for WT and T53D DAT, with a clearly altered response for T53A DAT (Fig. 6*A*), and regression analyses of the data revealed a significantly increased K_d for T53A DAT (196 ± 6 nM) relative to that of WT (30 ± 3 nM, $p < 0.01$) or T53D DATs (57 ± 6 nM, $p < 0.05$) (Fig. 6*B*). In Zn^{2+} experiments (Fig. 6*C*) the WT protein showed the expected stimulation of [^{3}H]CFT binding in the presence of Zn^{2+} (139 ± 10% of control, $p < 0.001$), whereas neither T53A nor T53D DATs showed responsiveness (both $p > 0.05$ *versus* vehicle, and $p < 0.01$ *versus* WT DAT plus Zn^{2+}). The inability of Zn^{2+} to rescue T53A binding indicates that reduced CFT affinity does not result from inward conformational bias, and suggests the binding pocket impacts result from enhanced inward and outward transitions.

Discussion

These findings demonstrate that phosphorylation of DAT Thr-53 is stimulated *in vitro* and *in vivo* by AMPH and METH, and mechanistically link modification of the site to control of DA transport, AMPH-induced DA efflux, and cocaine analog binding. Thr-53 is located near the intracellular end of TM1, which forms key contacts with DA and cocaine in the core active site, contains intracellular and extracellular gating residues, and is thought to undergo significant movements during substrate-driven transition from outwardly to inwardly facing conformations that open the translocation pathway (28, 29). Phosphorylation of Pro-directed residues adds negative charge to the site and also promotes *cis*-isomerization of the (S/T)-P peptide bond (30), generating a structure that likely possesses a distinct functionality from the *trans* form. The proximity of Thr-53 to TM1 thus suggests that regulation of transport functionalities could occur directly via charge or peptide backbone effects on helix conformation or gating properties. Thr-53 is also located within an SH3 domain that may dictate interactions with regulatory N-terminal binding partners (3) to induce effects.

The mechanisms underlying the effects of Thr-53 phosphorylation status on transport, efflux, and CFT binding will require further studies to clarify, as our findings of enhanced uptake, enhanced efflux, and reduced CFT affinity in T53A are not consistent with inward or outward conformational bias as has been invoked for other mutations. An alternative possibility could be that the increased uptake and efflux velocities of T53A follow from increased rates of transitioning between inward and outward forms, which would be consonant with Thr-53 phosphorylation reducing V_{max} by slowing these transitions (31). Reduced CFT affinity might thus result from impacts of these transitional alterations on binding pocket structure (32).

Although the identity of the kinase for Thr-53 remains unknown, Pro-directed motifs are specific for kinases such as MAPKs, CDKs, and glycogen-synthase kinases (33), indicating the potential for these pathways to provide functional input into reuptake and binding properties via this site. With the exception of ERK, few members of these kinase classes have been examined for regulation of DAT. DAT surface levels and uptake capacity are reduced by ERK inhibitors and increased by ERK-dependent signaling (34–36), and inhibition of ERK dampens receptor-mediated DA efflux (37) and affects AMPH

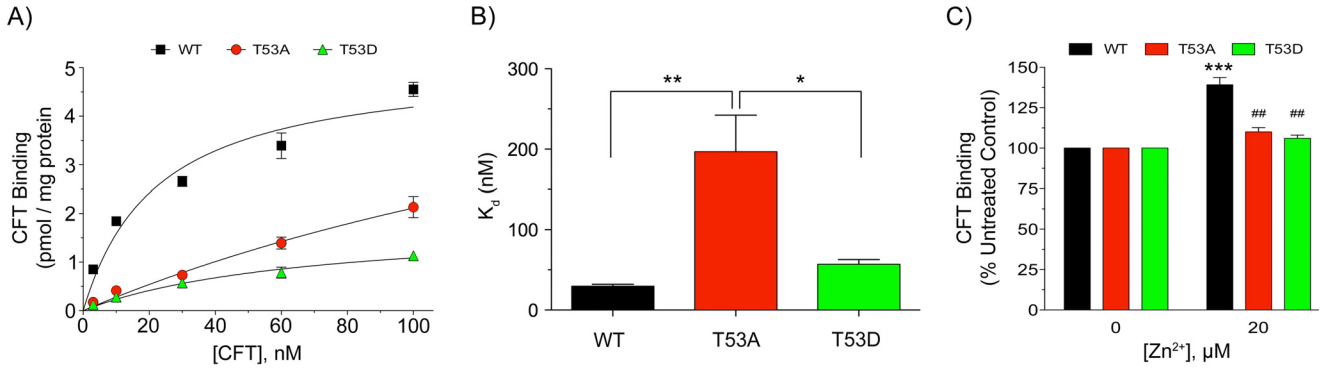

Figure 6. [^{3}H]CFT binding characteristics of Thr-53 mutants. WT, T53A, and T53D rDAT-LLCPK$_1$ cells were assessed for [^{3}H]CFT saturation binding (*A* and *B*), or Zn^{2+} effects on [^{3}H]CFT binding (*C*). *A,* [^{3}H]CFT saturation binding plots. Each point represents the mean ± S.E. of three independent experiments. *B,* K_d values obtained from plots in *A*. *, $p < 0.05$, T53A *versus* T53D; **, $p < 0.01$, T53A *versus* WT; WT *versus* T53D not significant (ANOVA followed by Tukey's post hoc test). *C,* cells were incubated with vehicle or 20 μM $ZnCl_2$ followed by analysis of [^{3}H]CFT binding. Values shown are mean ± S.E. of basal value for each form. ***, $p < 0.001$, Zn^{2+} *versus* vehicle; ##, $p < 0.01$, T53A and T53D DAT *versus* WT DAT at 20 μM Zn^{2+} (ANOVA followed by Tukey's post hoc test, $n = 5$).

behavioral outcomes that may be related to efflux (38). It is not known if any of these ERK effects are driven by *in vivo* phosphorylation of Thr-53, although ERK can phosphorylate Thr-53 *in vitro* (39) and is activated *in vivo* by systemic AMPH (38, 40). Indirect involvement of PKC in Thr-53-mediated processes is also a possibility, as PKC activators increase Thr-53 phosphorylation (16), likely by cross-talk with Pro-directed kinases (41), and AMPH stimulation of efflux is PKC-dependent (42).

With respect to Thr-53-mediated functions, we obtained unexpected differences from our previous study, finding elevated uptake and efflux V_{max} for T53A DAT and unchanged uptake and efflux V_{max} for T53D DAT, compared with our earlier findings that T53A and T53D DATs both possessed decreased transport and loss of AMPH-stimulated MPP^+ efflux (16). The different end points obtained in the two studies may thus arise from the different assessment methods used and will require further work to clarify, but importantly, our current findings demonstrate that phosphorylation of Thr-53 is not a mechanistic requirement for reverse transport.

Multiple methodological differences between perfusion and RDEV could factor into these differential outcomes, as perfusion is performed in attached cells, measures DA released by uncoupled ion influx as well as DA released by DAT operating in the exchange mode (43), and released DA is continuously removed, minimizing the extent of re-uptake, whereas RDEV is performed in cell suspension, only detects exchange-based DA efflux (21, 22), and DA is released into batch solution in which re-uptake can occur. Kinetic issues may also be key, as RDEV measurements are based on events occurring during the first 10 s after DA or AMPH addition, compared with radioisotope assays that measure events occurring over the course of minutes. The Thr-53 phosphorylation time course in our cell system indicates that fewer transporters would undergo AMPH-induced modification during RDEV analysis than in perfusion, which may establish different WT baselines used for comparisons to mutants. WT and mutant forms may also be regulated by time-dependent changes at other sites such as phosphorylation of Ser-7 or palmitoylation of Cys-580 (44) that may lead to differential outcomes depending on assay duration.

A final possibility underlying our different efflux findings could be the use of the endogenous substrate DA, which our study and a perfusion analysis (45) show can be released by T53A DAT, *versus* the exogenous compound MPP^+, which was not released by the Thr-53 mutants. The apparent affinity of DAT for MPP^+ is considerably lower than for DA (46, 47), and its reduced recognition and subsequent capacity for efflux may be exacerbated by Thr-53 mutation. These results may have implications for Thr-53 phosphorylation mechanisms in susceptibility of neurons to MPP^+ and other neurotoxic DAT substrates.

The findings that Thr-53 phosphorylation is stimulated by AMPH and METH but that T53A DAT exhibits elevated AMPH-stimulated DA efflux V_{max} suggests that phosphorylation of the site may dampen the initial rate of efflux. This contrasts with the enhancement of efflux driven by AMPH-stimulated phosphorylation of distal N-terminal serines (11, 12, 15), and indicates that overall efflux levels are established by integration of information from the two domains. Deciphering how this occurs will require further work, but could follow from differential kinase and phosphatase inputs or phosphorylation–dephosphorylation time courses. In this regard, AMPH/METH-stimulated Thr-53 phosphorylation in synaptosomes and the brain appears to occur more rapidly (1–10 min) than that of distal N-terminal phosphorylation (20–30 min) (12, 48), suggesting that the two domains may function as timers to control onset and suppression of efflux.

This study also adds to a growing body of evidence that supports regulation of cocaine binding to DAT by N-terminal phosphorylation. Mutagenesis and chimera studies have identified crucial roles for the N-terminal domain related to transporter conformational equilibrium and uptake blocker potencies (31, 49), and our findings that CFT affinity is reduced by phosphorylation-null mutations of Thr-53 and Ser-7 (13) and increased by conditions that stimulate phosphorylation of both sites (13, 16) indicates the ability of physiological inputs into the N terminus to confer rapid and reversible regulation of these functions. The potential for the increased affinity induced by Thr-53 phosphorylation to affect cocaine neurochemical and behavioral outcomes is supported by a recent finding that Thr-53 phosphorylation is elevated in conditions that promote enhanced cocaine potency and cocaine conditioned place preference (50).

Together these results provide strong evidence that Thr-53 phosphorylation functions to regulate uptake, efflux, and cocaine-binding properties of DAT, supporting the ability of this residue to control major functions in DA neurotransmission and psychostimulant drug mechanisms. Polymorphisms of DAT associated with bipolar and attention deficit hyperactivity disorders lead to dysregulation of uptake and efflux responses that are consistent with altered DA levels in pathologies (51). Signaling pathways that regulate proline-directed kinase pathways may thus provide major input on these functions via phosphorylation of Thr-53, and suggest this residue as a potential site for dysregulation in DA diseases and as a target for therapeutic manipulation of re-uptake.

Experimental procedures

Animals

Male Sprague-Dawley rats (175–300g) were purchased from Charles Rivers Laboratories (Wilmington, MA) and maintained in compliance with the guidelines established by the University of North Dakota Institutional Animal Care and Use Committee and the National Institutes of Health.

Reagents

CFT, (–)-cocaine, *d*-amphetamine, (+)-methamphetamine, dopamine, BZT, GBR 12909, mazindol, rimcazole, and Colorburst molecular mass markers were purchased from Sigma. [^{3}H]CFT (76 Ci/mmol) and [7,8-^{3}H]DA (45 Ci/mmol) were from PerkinElmer Life Sciences. Protein A–Sepharose resin was purchased from GE Healthcare Life Sciences. OA was purchased from Calbiochem/EMD Biosciences (La Jolla, CA), and all other chemicals were purchased from Sigma or Fischer Scientific (Pittsburg, PA).

Treatments in LLCPK$_1$ cells

LLCPK$_1$ (Lewis lung carcinoma porcine kidney) cells stably expressing the indicated forms of rDAT were maintained in α-minimum essential medium supplemented with 10% fetal bovine serum, 2 mM L-glutamine, 200 μg/ml of G418, and 100 μg/ml of penicillin/streptomycin in an incubation chamber with 5% CO_2, 95% O_2 at 37 °C. For phosphorylation experiments cells were plated in 6- or 12-well plates and grown to 70–80% confluence, washed twice with 1 or 2 ml of Krebs-Ringer HEPES (KRH) buffer (25 mM HEPES, 125 mM NaCl, 4.8 mM KCl, 1.2 mM KH_2PO_4, 1.3 mM $CaCl_2$, 1.2 mM $MgSO_4$, 5.6 mM glucose, pH 7.4), and treated with vehicle or the indicated concentrations of drugs for 30 min at 37 °C. At the end of treatment, cells were placed on ice, washed twice with ice-cold KRH, and lysed by adding RIPA buffer (1% Triton X-100, 1% sodium deoxycholate, 0.1% SDS, 125 mM sodium phosphate, 150 mM NaCl, 2 mM EDTA, 50 mM sodium fluoride) containing protease inhibitor. Samples were rocked on ice for 20 min and insoluble material was removed by centrifugation at 15,000 × *g* for 30 min at 4 °C.

Treatments in rat striatal synaptosomes

Striatal synaptosomes were prepared as previously described (19). Male Sprague-Dawley rats (175–300 g) were decapitated and the striatum was removed and weighed. Tissue was suspended in 10 ml of cold sucrose phosphate (SP) buffer (10 mM Na_2HPO_4, 0.32 M sucrose, pH 7.4) and homogenized in a Teflon-glass homogenizer. The homogenate was centrifuged at 3,000 × *g* for 3 min at 4 °C and the resulting supernatant was centrifuged at 17,000 × *g* for 12 min at 4 °C. The resulting P2 synaptosomal pellet was resuspended in SP buffer at 20–50 mg/ml of the original wet tissue weight. Synaptosomes were treated with vehicle, 10 μM AMPH, or 10 μM METH for the indicated times at 30 °C. Treatments were terminated by placing the sample at 4 °C and solubilizing tissue at 20 mg/ml of the original wet tissue weight with 0.5% SDS sample buffer (12).

In vivo treatments

Male Sprague-Dawley rats were injected subcutaneously with saline, METH (15 mg/kg), or cocaine (15 mg/kg), and caged separately for the duration of the experiment. At the end of the treatment time the animals were decapitated and striata were removed, weighed, and placed in ice-cold SP buffer. Tissue was disrupted with a Polytron homogenizer, and membranes were pelleted by centrifugation at 12,000 × *g* for 12 min at 4 °C and solubilized at 20 mg/ml of original wet tissue weight with 0.5% SDS sample buffer (12).

DAT immunoblotting and detection of Thr-53 phosphorylation

Lysates from cells, striatal synaptosomes, and striatal membranes were analyzed in duplicate for total DAT levels or Thr-53 phosphorylation as previously described (11, 16, 20). For analysis of total DAT, proteins were separated by SDS-PAGE on 4–20% gels and transferred to PVDF. Membranes were blocked with 3% BSA in PBS, incubated with MAb16 (1:1000), probed with alkaline phosphatase-conjugated anti-mouse IgG, and DAT bands were visualized via chemiluminescence. For analysis of Thr-53 phosphorylation, lysates were subjected to immunoprecipitation with pThr-53 Ab (16). Briefly, lysates were adjusted to 0.1% SDS with immunoprecipitation buffer (0.1% Triton X-100, 50 mM Tris-HCl, pH 8.0), and incubated for 2 h at 4 °C with affinity-purified polyclonal pThr-53 Ab covalently cross-linked to protein A–Sepharose resin. The resin was washed twice, and bound DATs were eluted with sample buffer (60 mM Tris, pH 6.8, 2% SDS, 10% glycerol, 100 mM DTT, 3% mercaptoethanol) and detected by immunoblotting with MAb16. DAT band intensities were quantified by densitometry using Quantity One (Bio-Rad) software and pThr-53 levels were normalized to the amount of total DAT protein and expressed relative to control samples set to 100%. Statistical significance was determined using ANOVA with Tukey's post hoc test or Student's *t* test with significance set at $p < 0.05$.

DA uptake and surface biotinylation

For analysis of AMPH potencies to inhibit [^{3}H]DA transport, WT and mutant rDAT-LLCPK$_1$ cells were grown to 70–80% confluence and uptake assays performed as described (16) with vehicle or the indicated concentrations of AMPH added simultaneously with DA, and transport values were converted to % control for each form. For analysis of DAT surface levels, cells were treated with vehicle, 0.5 μM DA, or 5 μM DA for 5 min and

subjected to surface biotinylation as described (16). For each form, the biotinylated bands were normalized to total DAT and expressed relative to WT control set at 100%. Statistical significance was determined using ANOVA with Tukey's post hoc test or Student's *t* test with significance set at $p < 0.05$.

RDEV

The general methods were as described previously (21–23). $LLCPK_1$ cells stably expressing WT, T53A, or T53D rDATs were cultured to confluence. Cells were harvested by trypsinization, washed with 1× PBS, and resuspended in 1.2 ml of KRH buffer (120 mM NaCl, 4.7 mM KCl, 2.2 mM $CaCl_2$, 1.2 mM $MgSO_4$, 1.2 mM KH_2PO_4, 10 mM HEPES, and 10 mM glucose, pH 7.4). Cell suspensions (300 μl) were added to the electrochemical chamber (kept at 37 °C) and the disk electrode was rotated at 4000 rpm for 5 min, sufficient for the assay temperature to stabilize. The oxidized DA current (+0.4 V *versus* Ag/AgCl reference electrode) was recorded every 300 ms by a National Instruments (Austin, TX) PC interface board. After 1 min of baseline signal acquisition, final concentrations of DA ranging from 0.25 to 10 μM were added to cell suspension to initiate the uptake measurement. Once the oxidized DA current was cleared to a plateau, AMPH was added at a final concentration of 10 μM to induce DA efflux. Recording was continued until no increase of oxidized DA current was observed, *i.e.* an elevated plateau was reached. The electrochemical chamber was washed 5 times with deionized water before carrying out the next assay. Protein levels in each assay were determined by the detergent compatible protein method (Bio-Rad). Initial DA uptake and efflux rates (pmol/s/mg) were calculated with the Origin Labtalk program at each tested DA concentration. Uptake and efflux kinetic parameters (K_m and V_{max}) were estimated by nonlinear fitting of the initial uptake or efflux rate to the initial added concentration of DA according to the Michaelis-Menten equation for saturation using Biosoft Kell Radlig software. The measurement of uptake and efflux in the same cell samples allowed us to make a correction for differences in efflux due to potential changes in uptake. It should be noted that at 10 μM AMPH, the concentration used to induce DA efflux, uptake of AMPH is saturated and determined only by its V_{max}. In RDEV, which measures exchange, efflux is proportional to uptake of inducer (21), which can vary depending on the mutation introduced in DAT. Assuming the V_{max} for AMPH uptake is proportional to that for DA uptake, we adopt the parameter V_{max} ratio, to normalize DA efflux: the ratio of V_{max} efflux over V_{max} uptake. Internal DA concentrations used for quantification of efflux kinetics are estimated as described.

[^{3}H]CFT binding

$LLCPK_1$ cells stably expressing the indicated DAT forms were washed with Hanks' balanced salt solution (5.33 mM KCl, 0.44 mM KH_2PO_4, 4.17 mM $NaHCO_3$, 137.93 mM NaCl, 0.34 mM Na_2HPO_4, and 5.56 mM glucose, pH 7.4). Cells were incubated with 1–100 nM CFT (each concentration 50% [^{3}H]CFT plus 50% unlabeled CFT) in KRH buffer for 2 h at 4 °C for saturation analysis, or incubated with 20 μM $ZnCl_2$ plus 5 nM [^{3}H]CFT for 2 h at 4 °C for Zn^{2+} response experiments. Binding was performed in triplicate with nonspecific binding determined using 10 μM mazindol. At the end of the incubation, cells were washed twice with KRH buffer, lysed with 1% Triton X-100, and samples were assessed for radioactivity by liquid scintillation counting. For saturation analyzes, B_{max} and K_d values were determined by nonlinear regression using Prism 3 software. For Zn^{2+} studies control binding values for each cell type were normalized to 100% and binding levels for treatment conditions were converted to percent control. Values were analyzed by ANOVA followed by Tukey's post hoc test with significance set at $p < 0.05$.

[^{3}H]DA efflux assay

WT and T53A rDAT $LLCPK_1$ cells were incubated at 37 °C with 10 nM [^{3}H]DA plus 3 μM DA for 15 min to load cells, followed by washing with ice-cold KRH to remove extracellular DA. Cells were then incubated for 5 min at 37 °C with 1 ml of KRH with or without 10 μM AMPH, and the entire volume was removed and counted to determine basal and stimulated DA efflux. Parallel sets of cells were assayed for cocaine-sensitive uptake, and efflux values are expressed as a fraction of the total amount of intracellular DA for each form.

Author contributions—S. C. performed experiments in Figs. 1–4, J. Z. performed experiments in Fig. 4 and Table 1, and M. E. S. performed experiments in Figs. 2, 4, 5, and 6. M. E. A. R., J. D. F., and R. A. V. conceived and monitored experiments and analyzed data. All authors contributed to writing of the manuscript.

Acknowledgment—The University of North Dakota was supported by the COBRE program of the National Center for Research Resources through Grant P20 GM104360 from the National Institutes of Health.

References

1. Giros, B., Jaber, M., Jones, S. R., Wightman, R. M., and Caron, M. G. (1996) Hyperlocomotion and indifference to cocaine and amphetamine in mice lacking the dopamine transporter. *Nature* **379,** 606–612
2. Sulzer, D. (2011) How addictive drugs disrupt presynaptic dopamine neurotransmission. *Neuron* **69,** 628–649
3. Vaughan, R. A., and Foster, J. D. (2013) Mechanisms of dopamine transporter regulation in normal and disease states. *Trends Pharm. Sci.* **34,** 489–496
4. Ramamoorthy, S., Shippenberg, T. S., and Jayanthi, L. D. (2011) Regulation of monoamine transporters: role of transporter phosphorylation. *Pharmacol. Ther.* **129,** 220–238
5. Bermingham, D. P., and Blakely, R. D. (2016) Kinase-dependent regulation of monoamine neurotransmitter transporters. *Pharmacol. Rev.* **68,** 888–953
6. Foster, J. D., and Vaughan, R. A. (2017) Phosphorylation mechanisms in dopamine transporter regulation. *J. Chem. Neuroanat.* **83–84,** 10–18
7. Kurian, M. A., Zhen, J., Cheng, S. Y., Li, Y., Mordekar, S. R., Jardine, P., Morgan, N. V., Meyer, E., Tee, L., Pasha, S., Wassmer, E., Heales, S. J., Gissen, P., Reith, M. E., and Maher, E. R. (2009) Homozygous loss-of-function mutations in the gene encoding the dopamine transporter are associated with infantile parkinsonism-dystonia. *J. Clin. Invest.* **119,** 1595–1603
8. Sakrikar, D., Mazei-Robison, M. S., Mergy, M. A., Richtand, N. W., Han, Q., Hamilton, P. J., Bowton, E., Galli, A., Veenstra-Vanderweele, J., Gill, M., and Blakely, R. D. (2012) Attention deficit/hyperactivity disorder-derived coding variation in the dopamine transporter disrupts microdomain targeting and trafficking regulation. *J. Neurosci.* **32,** 5385–5397
9. Bowton, E., Saunders, C., Erreger, K., Sakrikar, D., Matthies, H. J., Sen, N., Jessen, T., Colbran, R. J., Caron, M. G., Javitch, J. A., Blakely, R. D., and

Galli, A. (2010) Dysregulation of dopamine transporters via dopamine D2 autoreceptors triggers anomalous dopamine efflux associated with attention-deficit hyperactivity disorder. *J. Neurosci.* **30,** 6048–6057
10. Steinkellner, T., Yang, J. W., Montgomery, T. R., Chen, W. Q., Winkler, M. T., Sucic, S., Lubec, G., Freissmuth, M., Elgersma, Y., Sitte, H. H., and Kudlacek, O. (2012) Ca^{2+}/calmodulin-dependent protein kinase IIα (αCaMKII) controls the activity of the dopamine transporter: implications for Angelman syndrome. *J. Biol. Chem.* **287,** 29627–29635
11. Foster, J. D., Pananusorn, B., and Vaughan, R. A. (2002) Dopamine transporters are phosphorylated on N-terminal serines in rat striatum. *J. Biol. Chem.* **277,** 25178–25186
12. Cervinski, M. A., Foster, J. D., and Vaughan, R. A. (2005) Psychoactive substrates stimulate dopamine transporter phosphorylation and down-regulation by cocaine-sensitive and protein kinase C-dependent mechanisms. *J. Biol. Chem.* **280,** 40442–40449
13. Moritz, A. E., Foster, J. D., Gorentla, B. K., Mazei-Robison, M. S., Yang, J. W., Sitte, H. H., Blakely, R. D., and Vaughan, R. A. (2013) Phosphorylation of dopamine transporter serine 7 modulates cocaine analog binding. *J. Biol. Chem.* **288,** 20–32
14. Granas, C., Ferrer, J., Loland, C. J., Javitch, J. A., and Gether, U. (2003) N-terminal truncation of the dopamine transporter abolishes phorbol ester- and substance P receptor-stimulated phosphorylation without impairing transporter internalization. *J. Biol. Chem.* **278,** 4990–5000
15. Khoshbouei, H., Sen, N., Guptaroy, B., Johnson, L., Lund, D., Gnegy, M. E., Galli, A., and Javitch, J. A. (2004) N-terminal phosphorylation of the dopamine transporter is required for amphetamine-induced efflux. *PLos Biol.* **2,** E78
16. Foster, J. D., Yang, J. W., Moritz, A. E., Challasivakanaka, S., Smith, M. A., Holy, M., Wilebski, K., Sitte, H. H., and Vaughan, R. A. (2012) Dopamine transporter phosphorylation site threonine 53 regulates substrate reuptake and amphetamine-stimulated efflux. *J. Biol. Chem.* **287,** 29702–29712
17. Gray, C. H., and Barford, D. (2003) Getting in the ring: proline-directed substrate specificity in the cell cycle proteins Cdc14 and CDK2-cyclinA3. *Cell Cycle* **2,** 500–502
18. Lu, K. P., and Zhou, X. Z. (2007) The prolyl isomerase PIN1: a pivotal new twist in phosphorylation signalling and disease. *Nat. Rev. Mol. Cell Biol.* **8,** 904–916
19. Foster, J. D., and Vaughan, R. A. (2011) Palmitoylation controls dopamine transporter kinetics, degradation, and protein kinase C-dependent regulation. *J. Biol. Chem.* **286,** 5175–5186
20. Gaffaney, J. D., and Vaughan, R. A. (2004) Uptake inhibitors but not substrates induce protease resistance in extracellular loop two of the dopamine transporter. *Mol. Pharmacol.* **65,** 692–701
21. Chen, N., Trowbridge, C. G., and Justice, J. B., Jr. (1998) Voltammetric studies on mechanisms of dopamine efflux in the presence of substrates and cocaine from cells expressing human norepinephrine transporter. *J. Neurochem.* **71,** 653–665
22. Chen, N., and Justice, J. B. (2000) Differential effect of structural modification of human dopamine transporter on the inward and outward transport of dopamine. *Brain Res. Mol. Brain Res.* **75,** 208–215
23. Jones, K. T., Zhen, J., and Reith, M. E. (2012) Importance of cholesterol in dopamine transporter function. *J. Neurochem.* **123,** 700–715
24. Xie, T., McCann, U. D., Kim, S., Yuan, J., and Ricaurte, G. A. (2000) Effect of temperature on dopamine transporter function and intracellular accumulation of methamphetamine: implications for methamphetamine-induced dopaminergic neurotoxicity. *J. Neurosci.* **20,** 7838–7845
25. Forrest, L. R., Zhang, Y. W., Jacobs, M. T., Gesmonde, J., Xie, L., Honig, B. H., and Rudnick, G. (2008) Mechanism for alternating access in neurotransmitter transporters. *Proc. Natl. Acad. Sci. U.S.A.* **105,** 10338–10343
26. Beuming, T., Shi, L., Javitch, J. A., and Weinstein, H. (2006) A comprehensive structure-based alignment of prokaryotic and eukaryotic neurotransmitter/Na^+ symporters (NSS) aids in the use of the LeuT structure to probe NSS structure and function. *Mol. Pharmacol.* **70,** 1630–1642
27. Norgaard-Nielsen, K., and Gether, U. (2006) Zn^{2+} modulation of neurotransmitter transporters. *Handb. Exp. Pharmacol.* **2006,** 1–22
28. Kniazeff, J., Shi, L., Loland, C. J., Javitch, J. A., Weinstein, H., and Gether, U. (2008) An intracellular interaction network regulates conformational transitions in the dopamine transporter. *J. Biol. Chem.* **283,** 17691–17701
29. Krishnamurthy, H., and Gouaux, E. (2012) X-ray structures of LeuT in substrate-free outward-open and apo inward-open states. *Nature* **481,** 469–474
30. Lu, K. P., Liou, Y. C., and Zhou, X. Z. (2002) Pinning down proline-directed phosphorylation signaling. *Trends Cell Biol.* **12,** 164–172
31. Guptaroy, B., Zhang, M., Bowton, E., Binda, F., Shi, L., Weinstein, H., Galli, A., Javitch, J. A., Neubig, R. R., and Gnegy, M. (2009) A juxtamembrane mutation in the N terminus of the dopamine transporter induces preference for an inward-facing conformation. *Mol. Pharmacol.* **75,** 514–524
32. Dehnes, Y., Shan, J., Beuming, T., Shi, L., Weinstein, H., and Javitch, J. A. (2014) Conformational changes in dopamine transporter intracellular regions upon cocaine binding and dopamine translocation. *Neurochem. Int.* **73,** 4–15
33. Ubersax, J. A., and Ferrell, J. E., Jr. (2007) Mechanisms of specificity in protein phosphorylation. *Nat. Rev. Mol. Cell Biol.* **8,** 530–541
34. Morón, J. A., Zakharova, I., Ferrer, J. V., Merrill, G. A., Hope, B., Lafer, E. M., Lin, Z. C., Wang, J. B., Javitch, J. A., Galli, A., and Shippenberg, T. S. (2003) Mitogen-activated protein kinase regulates dopamine transporter surface expression and dopamine transport capacity. *J. Neurosci.* **23,** 8480–8488
35. Bolan, E. A., Kivell, B., Jaligam, V., Oz, M., Jayanthi, L. D., Han, Y., Sen, N., Urizar, E., Gomes, I., Devi, L. A., Ramamoorthy, S., Javitch, J. A., Zapata, A., and Shippenberg, T. S. (2007) D2 receptors regulate dopamine transporter function via an extracellular signal-regulated kinases 1 and 2-dependent and phosphoinositide 3 kinase-independent mechanism. *Mol. Pharmacol.* **71,** 1222–1232
36. Thompson, A. C., Zapata, A., Justice, J. B., Jr, Vaughan, R. A., Sharpe, L. G., and Shippenberg, T. S. (2000) κ-Opioid receptor activation modifies dopamine uptake in the nucleus accumbens and opposes the effects of cocaine. *J. Neurosci.* **20,** 9333–9340
37. Alyea, R. A., and Watson, C. S. (2009) Nongenomic mechanisms of physiological estrogen-mediated dopamine efflux. *BMC Neurosci.* **10,** 59
38. Shi, X., and McGinty, J. F. (2006) Extracellular signal-regulated mitogen-activated protein kinase inhibitors decrease amphetamine-induced behavior and neuropeptide gene expression in the striatum. *Neuroscience* **138,** 1289–1298
39. Gorentla, B. K., Moritz, A. E., Foster, J. D., and Vaughan, R. A. (2009) Proline-directed phosphorylation of the dopamine transporter N-terminal domain. *Biochemistry* **48,** 1067–1076
40. Mao, L. M., Reusch, J. M., Fibuch, E. E., Liu, Z., and Wang, J. Q. (2013) Amphetamine increases phosphorylation of MAPK/ERK at synaptic sites in the rat striatum and medial prefrontal cortex. *Brain Res.* **1494,** 101–108
41. Rozengurt, E. (2007) Mitogenic signaling pathways induced by G protein-coupled receptors. *J. Cell Physiol.* **213,** 589–602
42. Johnson, L. A., Guptaroy, B., Lund, D., Shamban, S., and Gnegy, M. E. (2005) Regulation of amphetamine-stimulated dopamine efflux by protein kinase Cβ. *J. Biol. Chem.* **280,** 10914–10919
43. Sitte, H. H., Huck, S., Reither, H., Boehm, S., Singer, E. A., and Pifl, C. (1998) Carrier-mediated release, transport rates, and charge transfer induced by amphetamine, tyramine, and dopamine in mammalian cells transfected with the human dopamine transporter. *J. Neurochem.* **71,** 1289–1297
44. Moritz, A. E., Rastedt, D. E., Stanislowski, D. J., Shetty, M., Smith, M. A., Vaughan, R. A., and Foster, J. D. (2015) Reciprocal phosphorylation and palmitoylation control dopamine transporter Kinetics. *J. Biol. Chem.* **290,** 29095–29105
45. Wang, Q., Bubula, N., Brown, J., Wang, Y., Kondev, V., and Vezina, P. (2016) PKC phosphorylates residues in the N-terminal of the DA transporter to regulate amphetamine-induced DA efflux. *Neurosci. Lett.* **622,** 78–82
46. Kitayama, S., Mitsuhata, C., Davis, S., Wang, J. B., Sato, T., Morita, K., Uhl, G. R., and Dohi, T. (1998) MPP^+ toxicity and plasma membrane dopamine transporter: study using cell lines expressing the wild-type and mutant rat dopamine transporters. *Biochim. Biophys. Acta* **1404,** 305–313

47. Brüss, M., Wieland, A., and Bönisch, H. (1999) Molecular cloning and functional expression of the mouse dopamine transporter. *J. Neural. Transm.* **106,** 657–662
48. Vaughan, R. A., Huff, R. A., Uhl, G. R., and Kuhar, M. J. (1997) Protein kinase C-mediated phosphorylation and functional regulation of dopamine transporters in striatal synaptosomes. *J. Biol. Chem.* **272,** 15541–15546
49. Sweeney, C. G., Tremblay, B. P., Stockner, T., Sitte, H. H., and Melikian, H. E. (2017) Dopamine transporter amino- and carboxy-termini synergistically contribute to substrate and inhibitor affinities. *J. Biol. Chem.* **292,** 1302–1309
50. Calipari, E. S., Juarez, B., Morel, C., Walker, D. M., Cahill, M. E., Ribeiro, E., Roman-Ortiz, C., Ramakrishnan, C., Deisseroth, K., Han, M. H., and Nestler, E. J. (2017) Dopaminergic dynamics underlying sex-specific cocaine reward. *Nat. Commun.* **8,** 13877
51. Hahn, M. K., and Blakely, R. D. (2007) The functional impact of SLC6 transporter genetic variation. *Annu. Rev. Pharmacol. Toxicol.* **47,** 401–441